This article was downloaded by:
On: *25 January 2011*
Access details: *Access Details: Free Access*
Publisher *Taylor & Francis*
Informa Ltd Registered in England and Wales Registered Number: 1072954 Registered office: Mortimer House, 37-41 Mortimer Street, London W1T 3JH, UK

Separation Science and Technology

Publication details, including instructions for authors and subscription information:
http://www.informaworld.com/smpp/title~content=t713708471

Porosimetric Characterization of Inorganic Membranes

A. Bottino[a]; G. Capannelli[a]; A. Grosso[a]; O. Monticelli[a]; M. Nicchia[a]
[a] ISTITUTO DI CHIMICA INDUSTRIALE UNIVERSITÀ DI GENOVA, GENOA, ITALY

To cite this Article Bottino, A. , Capannelli, G. , Grosso, A. , Monticelli, O. and Nicchia, M.(1994) 'Porosimetric Characterization of Inorganic Membranes', Separation Science and Technology, 29: 8, 985 — 999
To link to this Article: DOI: 10.1080/01496399408005612
URL: http://dx.doi.org/10.1080/01496399408005612

PLEASE SCROLL DOWN FOR ARTICLE

Full terms and conditions of use: http://www.informaworld.com/terms-and-conditions-of-access.pdf

This article may be used for research, teaching and private study purposes. Any substantial or systematic reproduction, re-distribution, re-selling, loan or sub-licensing, systematic supply or distribution in any form to anyone is expressly forbidden.

The publisher does not give any warranty express or implied or make any representation that the contents will be complete or accurate or up to date. The accuracy of any instructions, formulae and drug doses should be independently verified with primary sources. The publisher shall not be liable for any loss, actions, claims, proceedings, demand or costs or damages whatsoever or howsoever caused arising directly or indirectly in connection with or arising out of the use of this material.

SEPARATION SCIENCE AND TECHNOLOGY, **29**(8), pp. 985–999 1994

Porosimetric Characterization of Inorganic Membranes

A. BOTTINO, G. CAPANNELLI, A. GROSSO, O. MONTICELLI
and M. NICCHIA
ISTITUTO DI CHIMICA INDUSTRIALE
UNIVERSITA DI GENOVA
CORSO EUROPA 30, I-16132, GENOA, ITALY

ABSTRACT

This paper deals with the evaluation of pore size and pore size distribution of inorganic membranes by liquid–liquid displacement porometry. Carbon and ceramic membranes were tested with a fully automatic porometer, and different results were obtained depending on the type of membrane. Membranes were also examined with the aid of a scanning electron microscope. The results of porosimetric measurements are discussed in conjunction with those of microscopic observations.

INTRODUCTION

The use of porous inorganic membrane in conventional separation processes such as ultra and microfiltration, as well as in membrane reactor technology, has gained increased interest in recent years (1–3). The success in the application depends not only on membrane flux but also on membrane selectivity, which is mainly related to pore size and pore-size distribution. Therefore, the measurement of these parameters is of paramount importance for choosing the most appropriate membrane for each application.

Inorganic membranes are generally made of ceramic or carbon, and as far as their porous structure is concerned, can be classified as "symmetric," with an even porosity over the membrane cross-section, or "asymmetric," with a porosity gradually increasing from the top to the bottom surface of the membrane.

In porosimetric characterization of a membrane, only the evaluation of open pores is of practical interest. In addition, in the case of an asymmetric membrane, only knowledge of size and size distribution of the pores in the top surface is necessary.

For these reasons, methods based on nitrogen adsorption and mercury penetration which are routinely used for porosimetric characterization of finely porous materials, such as, for example, ceramic and catalysts, have a limited application in the membrane field whereas special techniques, such as permporometry, gas–liquid, and liquid–liquid displacement porometry, have been developed.

Permporometry (4–11) involves the use of a mixture of a condensable organic vapor, for instance, ethanol or carbon tetrachloride, and an incondensable gas, for instance, nitrogen or helium. The organic vapor is condensed in the membrane pores by progressively increasing the relative vapor pressure, and the flow of the incondensable gas through empty membrane pores is simultaneously measured. Pore-size distribution is calculated from relative pressure data using the Kelvin equation (12). Permporometry covers the range from a few nanometers to a 50-nm pore radius.

Gas–liquid displacement porometry (GLPD) (13, 14) originates from the well-known bubble-pressure method (15, 16). This consists in applying an increasing gas pressure to one side of a membrane sample completely filled with a liquid, for instance, water, and measuring the pressure at which the first bubble is observed on the other side. From this pressure, P, the pore radius, r, can be calculated using the Cantor equation:

$$P = \frac{2\gamma}{r} \cos \theta$$

where γ is the surface tension and θ is the contact angle, which is generally assumed to be zero.

Indeed, this method provides only a measure of the radius of the largest pore since the gas passes through it first. After the bubble point is reached, smaller pores are emptied with further increases in the pressure, thus becoming available for gas permeation. In the GLDP the gas flow, J, through emptied pores is measured as a function of the applied pressure, P. From these measurements, pore-size distribution can be obtained. In fact, the experimental flow vs pressure curve can be directly converted into the flow (or permeability, $L = J/P$) vs pore radius curve by using the Cantor equation. Moreover, it can be used to obtain the pore number vs pore radius curve. This is done by considering the Hagen–Poiseuille equation:

$$J = \frac{n\pi r^4 P}{8\eta l}$$

where n is the number of pores, η is the gas viscosity, and l is the pore length.

Because of the high gas–liquid surface tension, high gas pressures must be used to force the wetting liquid out of very small membrane pores. This can be clearly seen in Table 1 where the pressure values for three given pore sizes and different air–liquid pairs are reported. For this reason, pore-size distributions by GLDP are generally limited to pore size of not less than about 50 μm.

Liquid–liquid displacement porometry (LLDP) (7, 17–21) has the same basis as the aforementioned method, but a liquid is used as the displacing medium instead of a gas. Table 2 lists a number of pairs of immiscible liquids which are generally employed to perform LLDP measurements. As can be seen, these pairs are characterized by low interfacial tension values. Therefore, it becomes possible to evaluate very small pores, e.g., those in the nanometer range, without applying high pressure that, especially in the case of a polymeric membrane, can densify the membrane structure, thus leading to unreliable porosimetric results.

TABLE 1
Pressure vs Pore Radius Relationship[a] for a Given Air–Wetting Liquid Pair

Wetting liquid	Surface tension[b] (mN/m)	Pressure (MPa) for pore radius shown		
		1 μm	0.1 μm	10 nm
Fluorinerts[c]	12–18[d]	0.024–0.036	0.24–0.36	2.4–3.6
n-Hexane	18.4	0.0368	0.368	3.68
Isopropanol	21.7	0.0434	0.434	5.34
Methanol	22.6	0.0452	0.452	4.52
Chloroform	27.1	0.0542	0.542	5.42
Benzene	28.9	0.0578	0.578	5.78
Formamide	58.2	0.1160	1.160	11.60
Water	72.8	0.1460	1.460	14.60

[a] Complete wetting is assumed ($\cos \theta = 1$).
[b] Values at 20°C.
[c] Perfluorocarbons. Registered trademarks of 3M.
[d] Depends on the type.

TABLE 2
Pressure vs Pore Radius Relationship[a] for a Given Wetting Liquid[b]-Displacing Liquid Pair

Displacing liquid	Surface tension[c] (mN/m)	Pressure (MPa) for pore radius shown		
		1 μm	100 μm	1 nm
Alcohol mixture[d]	0.35	0.70×10^{-3}	0.70×10^{-2}	0.7
Isobutanol	1.7	3.40×10^{-3}	3.4×10^{-2}	3.4
1-Pentanol	4.8	9.60×10^{-3}	9.6×10^{-2}	9.6
1-Octanol	8.5	1.70×10^{-2}	0.17	17
Diethyl ether	10.7	2.14×10^{-2}	0.214	21.4
Benzene	35.0	0.070	0.70	70
Carbon tetrachloride	45.0	0.070	0.90	90
n-Heptane	51.0	0.102	1.02	102

[a] Complete wetting is assumed.

[b] Water except for alcohol mixture.[d]

[c] Values at 20°C.

[d] Alcohol-rich phase from the phase demixing of a mixture of water–methanol–isobutanol (25/7/15 v/v). The water-rich phase is used as membrane-wetting liquid (see text).

LLDP attracted our attention at the beginning of the 1980s (22). Since that time this method has been progressively refined and a porometer has been developed to automatically perform flow vs pressure measurements, store and elaborate all the data, and finally print porosity results either as a table or as a plot (23, 24). A particular feature of the porometer is its mode of operation which consists of increasing stepwise the flow of the displacing liquid by means of a HPLC volumetric pump and measuring the corresponding pressure drop across the membrane. This overcomes the difficulty of measuring very low flows, e.g., of the order of a few μL/min, as these are set and controlled by the HPLC pump.

For a reason mainly connected to our activity in the preparation of polymeric membranes, the porometer has been till now only applied to flat-sheet membranes made of these materials (25–28). On the basis of the increasing application of inorganic membranes and recognizing the need for new and better methods for evaluating their porosimetric characteristics, a study has been recently undertaken to extend the use of the porometer to these types of membranes. In this paper, porosimetric data of carbon and ceramic membranes are reported and discussed in conjunction with the results obtained from scanning electron microscope observations of the membrane surfaces.

EXPERIMENTAL

Membranes

Ceramic and carbon membranes were in the form of tubes with an outer diameter of ≈ 10 mm and an inner diameter of ≈ 6 mm. Both types of membranes were supplied by a French firm, the name of which is not reported here because of a secret agreement with the manufacturer.

Chemicals

Methanol and isobutanol were of reagent grade and were used as received without further purification. Distilled deionized water was further purified by reverse osmosis treatment prior to use.

Preparation of the Liquid Mixture for LLDP Measurements

Freshly purified water (250 mL), methanol (70 mL), and isobutanol (150 mL) were poured into a flask and stirred for 20–30 minutes. The resulting mixture was then transferred to a separatory funnel and allowed to stand overnight. The separated aqueous-rich phase was drained off and stored in a stoppered bottle until used for membrane impregnation. The alcohol-rich phase was transferred to the porometer reservoir to be used as the displacing medium. All operations were carried out in a conditioned room at 20°C.

LLDP Measurements

Porosimetric measurements were performed at 20°C. The kinematic viscosity of the alcohol-rich phase at this temperature was $\eta = 3.4 \times 10^{-3}$ Pa·s (24). The interfacial tension value of the two immiscible phases is given in Table 2.

Scanning Electron Microscope (SEM) Observations

The surface and the cross section of the membranes were first coated with gold by means of an Agar Aids sputter coater and then observed with the aid of a Cambridge Stereoscan 250 Mk2 scanning electron microscope.

RESULTS AND DISCUSSION

Design and Development of End-Fittings

The use of membranes with tubular configurations required the design and the development of end-fittings capable of providing proper hydraulic connections between membranes tubes and the porometer. Two different methods were followed. The first one (Fig. 1) consisted of coating each end of the membrane tube (1) with an epoxy resin (2) which sealed the surface and at the same time bonded the membrane tube to the metal body (3). This latter had a screwed part at one end to which the 1/16″ o.d. tube (5) of the HPLC pump of the porometer was connected by means of a standard compression screw (4). An important parameter for the success of the method was the initial viscosity of the resin. In fact, if the viscosity was too low, the resin wet the tube for a certain extent (because of the capillarity phenomenon) with consequent membrane pore clogging, while if the initial viscosity was too high, adhesion problems between the solidified resin and the membrane tube occurred. The second method (Fig. 2) involved the installation at each of the membrane ends of an O-ring (6) which was then squeezed by tightening the metal nut (7). With this method it was first necessary to make the membrane end impermeable. This was done with a polyimide coating (2) (Pyralin, Du Pont de Nemours) selected on the basis of its excellent chemical resistance. In order to obtain a proper coating, the end of the membrane was first immersed in the polymer solution and then removed and held in a vertical position to drain excess solution from the inside and outside surfaces of the tube. The coated solution was dried by a jet of air at 100°C and crosslinked by heat curing in an oven at 300°C.

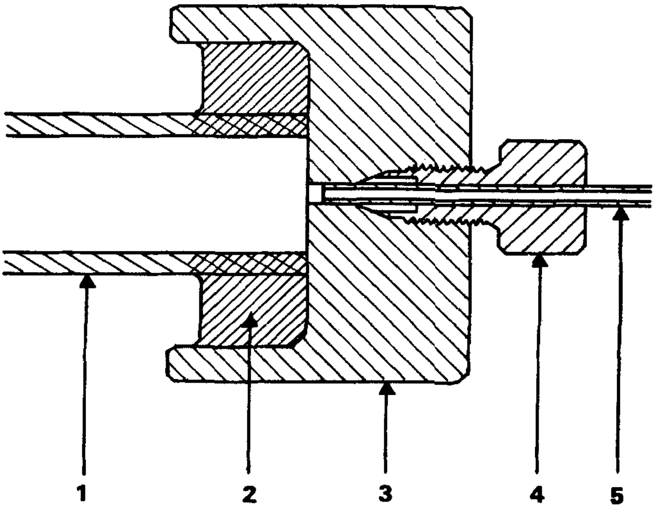

FIG. 1 Schematic drawing of the membrane end-fitting: (1) membrane tube, (2) epoxy resin, (3) body, (4) compression screw, (5) porometer tube.

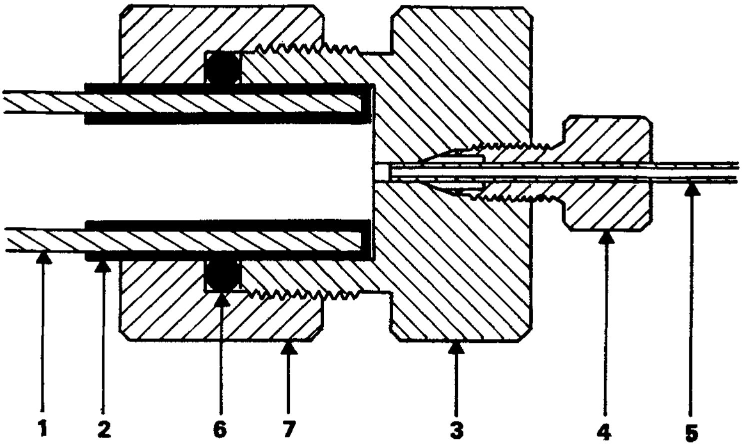

FIG. 2 Schematic drawing of the membrane end-fitting: (1) membrane tube, (2) polyimide coating, (3) body, (4) compression screw, (5) porometer tube, (6) O-ring, (7) nut.

Of the two methods described here, the second one was generally adopted since it was less time consuming and allowed quicker reuse of the end-fittings.

Porosimetric Measurements and SEM Observations

Figure 3 shows SEM micrographs taken at different magnifications of the cross section of the carbon membrane. As can be seen, the membrane exhibits a symmetric structure composed of aggregates of particles; the size of such particles does not change over the cross section. Figure 4 shows a SEM micrograph of the surface of the membrane. By comparing this figure with Figs. 3(b) and 3(c), no substantial differences in the morphologies can be seen.

Porosimetric results of the carbon membrane are reported in Figs. 5 and 6. It is worthwhile to remember that the pore permeability vs pore radius distribution (Fig. 5) directly derives from the experimental flux and pressure data while the pore number vs pore radius distribution (Fig. 6) is obtained by using the Hagen–Poiseuille equation as a transport model. Two main families of pores (*a* and *b*) can be clearly observed from these figures. By comparing the porosimetric results with the SEM micrograph shown in Fig. 4, it could be reasonable to connect Family *b* to the large voids between the aggregates. As far as Family *a* is concerned, obviously no information can be obtained from Fig. 4. However, it can be assumed that such families relate to the microvoids between particles. It is interesting to observe that by using GLDP or permporometry to test the same

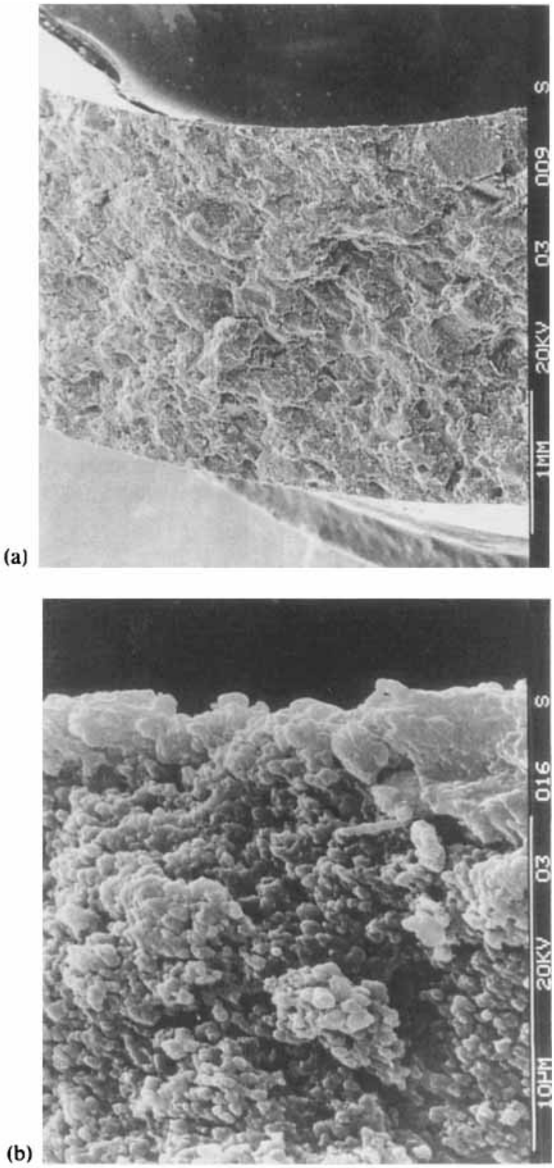

FIG. 3 SEM micrographs of the cross section of the carbon membrane: (a) overall cross-section; (b) upper part of (a); (c) upper part of (b).

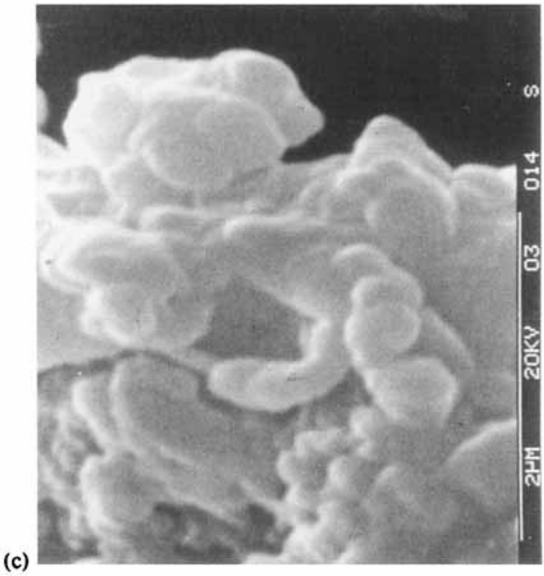

FIG. 3 Continued

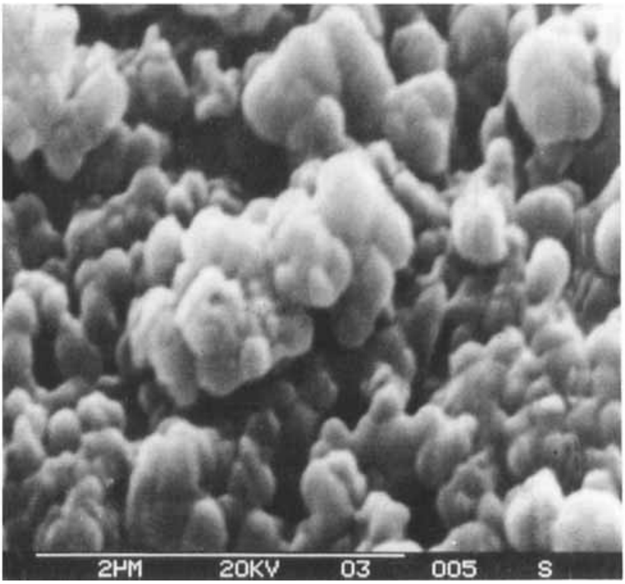

FIG. 4 SEM micrograph of the surface of the carbon membrane.

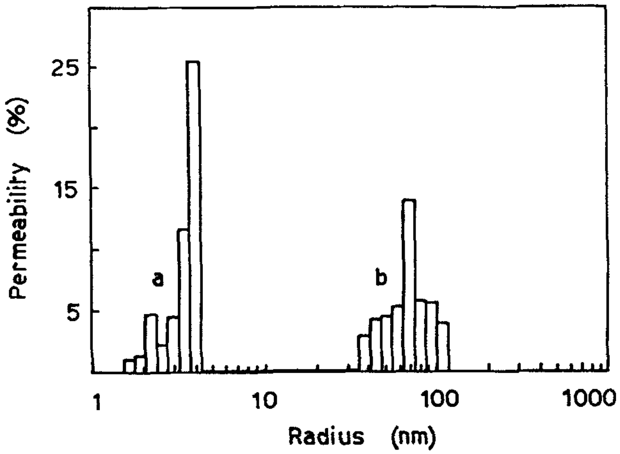

FIG. 5 Percent pore permeability vs pore radius for the carbon membrane.

membrane, one can obtain only partial information because the former method cannot be applied to pores with of less than 50 nm while the latter is used to detect pores with radii up to 50 nm.

Scanning electron micrographs of the cross section of the ceramic membrane are shown in Fig. 7. The contrast between these micrographs and those reported in Fig. 3 is striking. The structure of the ceramic membrane

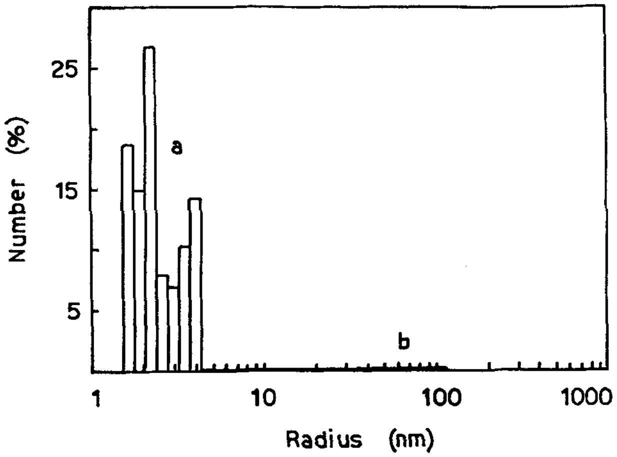

FIG. 6 Percent pore number vs pore radius for the carbon membrane.

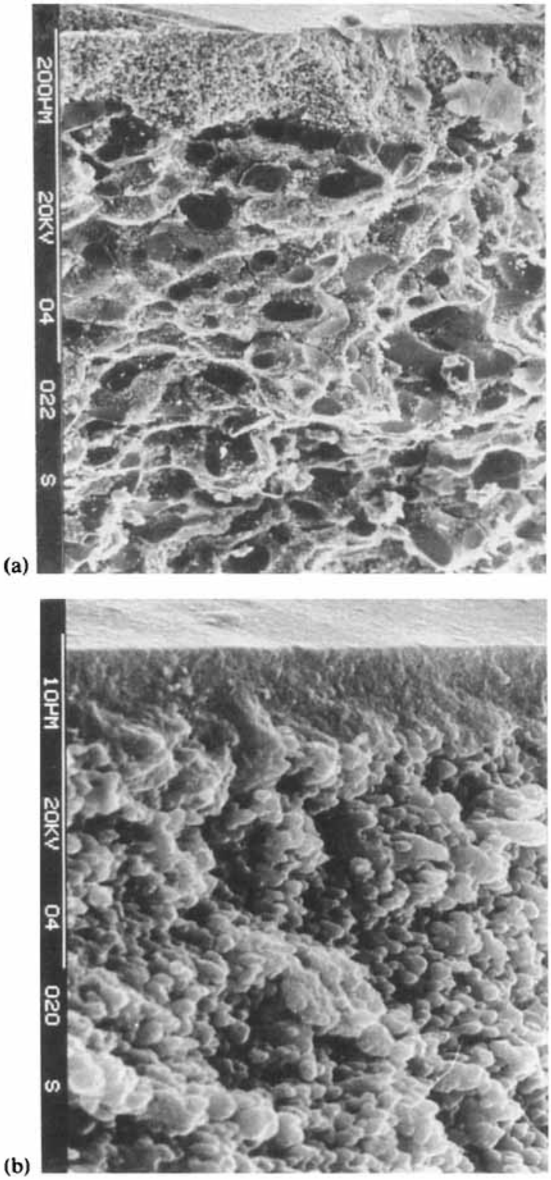

FIG. 7 SEM micrographs of the cross section of the ceramic membrane: (a) upper part of the membrane cross-section; (b) upper part of (a); (c) upper part of (b).

(c)

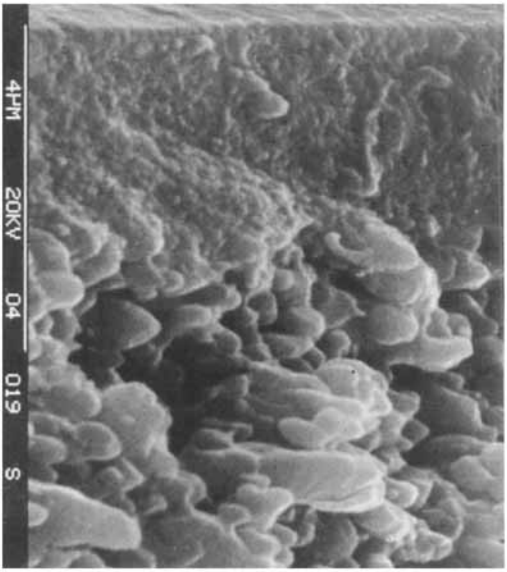

FIG. 7 Continued

is asymmetric, and three well-distinguishable layers are present: a compact surface thin layer (Fig. 7c), an intermediate layer composed of well-defined particles (Fig. 7b), and a thick bottom layer where large voids appear (Fig. 7a). Inspection of the high-magnification SEM micrograph in Fig. 8 reveals a rather smooth surface without any apparent porosity.

The results of porosimetric measurements are reported in Figs. 9 and 10. They refer to the porosity of the surface thin layer and indicate a very narrow pore size distribution, with pores in the range of 1 nm. These results are in agreement with those of the SEM observation (Fig. 8).

CONCLUSIONS

LLDP has proven to be a useful technique for investigating the porosity of inorganic membranes. LLDP represents a valid alternative to GLDP and permporometry, especially because it allows pores to be studied over a wide range of sizes. The porosimetric results obtained indicate a unimodal pore-size distribution for the ceramic membrane and a bimodal one

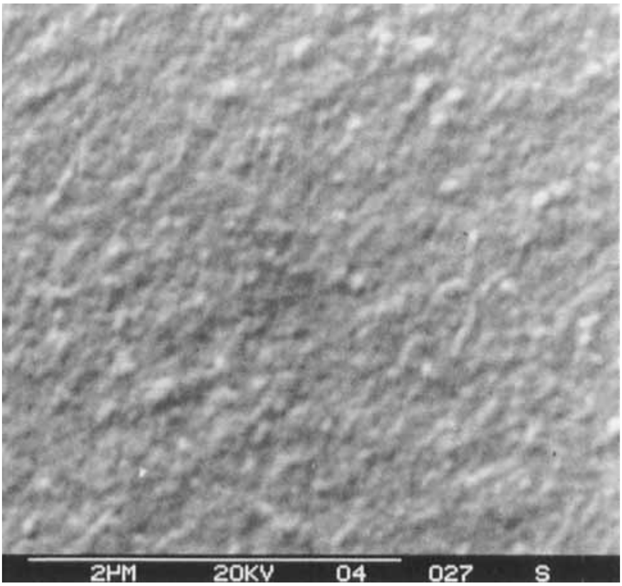

FIG. 8 SEM micrograph of the surface of the ceramic membrane.

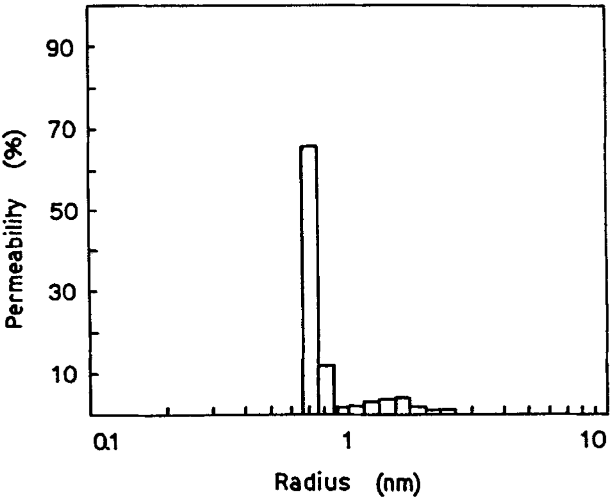

FIG. 9 Percent pore permeability vs pore radius for the ceramic membrane.

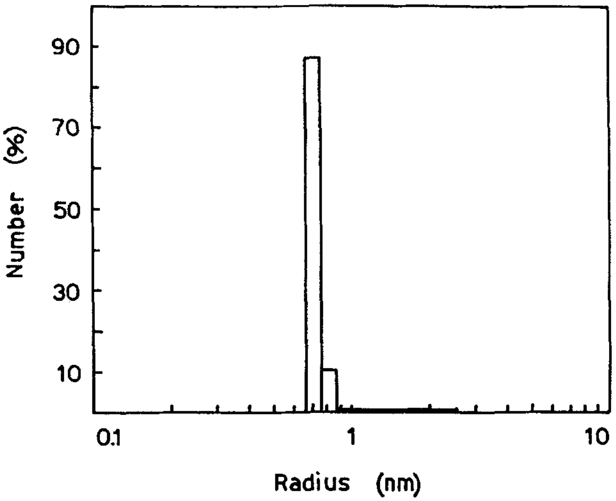

FIG. 10 Percent pore number vs pore radius for the ceramic membrane.

for the carbon membrane. These results seem to be consistent with those of SEM observations.

ACKNOWLEDGMENTS

This work was financially supported by Ministero dell'Università e della Ricerca Scientifica e Tecnologica (quota 60%) and by Consiglio Nazionale delle Ricerche (Progetto Finalizzato Chimica Fine II), Rome, Italy.

REFERENCES

1. *Proceedings of the 1st International Conference on Inorganic Membranes, ICIM 89*, Montpellier, France, July 3–6, 1989.
2. *Proceedings of the 2nd International Conference on Inorganic Membranes, ICIM$_2$-91*, Montpellier, France, July 1–4, 1991.
3. H. P. Hsieh, *Catal. Rev., Sci. Eng., 33*, 70 (1991).
4. C. Eyraud, M. Betempts, and J. F. Quinson, *Bull. Soc. Chim. Fr., 9–10*, I-238 (1984).
5. A. Mey-Marom and M. G. Katz, *J. Membr. Sci., 27*, 119 (1986).
6. M. Katz and G. Baruch, *Desalination, 58*, 199 (1986).
7. C. Eyraud, *Thermochim. Acta, 100*, 223 (1986).
8. C. Eyraud, J. F. Quinson, and M. Brun, in *Characterization of Porous Solids* (K. K. Unger et al., Eds.), Elsevier, Amsterdam, 1988, p. 295.
9. C. Eyraud and C. Jallut, *Proceedings of the 1st International Conference on Inorganic Membranes, ICIM 89*, Montpellier, France, July 3–6, 1989, p. 193.

10. D. E. Fain, in *Proceedings of the 1st International Conference on Inorganic Membranes, ICIM 89*, Montpellier, France, July 3–6, 1989, p. 199.
11. F. P. Cuperus, D. Bargeman, and C. A. Smolders, *J. Membr. Sci.*, *71*, 57 (1992).
12. S. J. Gregg and K. S. W. Sing, *Adsorption, Surface Area and Porosity*, 2nd ed., Academic Press, New York, 1982.
13. R. A. Weuman and B. V. Miller, *Particle Size Analysis*, Wiley, New York, 1985.
14. W. Kuyawski, P. Adamczak, and A. Narebska, *Sep. Sci. Technol.*, *24*, 495 (1989).
15. ASTM F-316 (1980).
16. T. D. Brock, *Membrane Filtration: A User's Guide and Reference Manual*, Science Tech Inc, Madison, Wisconsin, 1983.
17. F. Erbe, *Kolloid Z.*, *63*, 277 (1933).
18. P. Grabar and S. Nikitine, *J. Chim. Phys.*, *33*, 721 (1936).
19. V. Hampl and S. Spurny, *Collect. Czech. Chem. Commun.*, *32*, 4181 (1967).
20. R. E. Kesting, *Synthetic Polymeric Membranes*, 2nd ed., Wiley, New York, 1985.
21. M. G. Lin, R. Ben Aim, and M. Mietton Peuchot, in *Proceedings of the 2nd International Conference on Inorganic Membranes, ICIM$_2$-91*, Montpellier, France, July 1–4, 1991, p. 603.
22. G. Capannelli, F. Vigo, and S. Munari, *J. Membr. Sci.*, *15*, 289 (1983).
23. S. Munari, A. Bottino, G. Capannelli, and P. Moretti, *Desalination*, *53*, 11 (1985).
24. G. Capannelli, I. Becchi, A. Bottino, P. Moretti, and S. Munari, in *Characterization of Porous Solids* (K. K. Unger et al., ed.), Elsevier, Amsterdam, 1988, p. 283.
25. S. Munari, A. Bottino, G. Capannelli, P. Moretti, and P. Petit Bon, *Desalination*, *70*, 265 (1988).
26. S. Munari, A. Bottino, P. Moretti, G. Capannelli, and I. Becchi, *J. Membr. Sci.*, *41*, 69 (1989).
27. P. Abaticchio, A. Bottino, G. Camera Roda, G. Capannelli, and S. Munari, *Desalination*, *78*, 235 (1990).
28. A. Bottino, G. Capannelli, P. Petit Bon, M. Cao, M. Pegoraro, and G. Zoia, *Sep. Sci. Technol.*, *26*, 1315 (1991).

Received by editor September 14, 1992